ISSN 1674-1056
http://cpb.iphy.ac.cn
http://iopscience.iop.org/cpb
中国物理 B
Chinese Physics
中国物理 Chinese Physics B

Ultra-thin circularly polarized lens antenna based on single-layered transparent metasurface

Kaiyue Liu(刘凯越), Guangming Wang(王光明), Tong Cai(蔡通), Wenlong Guo(郭文龙), Yaqiang Zhuang(庄亚强), Gang Liu(刘刚)

Citation: Chin. Phys. B . 2018, 27(8): 084101. **doi:** 10.1088/1674-1056/27/8/084101

Journal homepage: http://cpb.iphy.ac.cn; http://iopscience.iop.org/cpb

What follows is a list of articles you may be interested in

Reliable approach for bistatic scattering of three-dimensional targets from underlying rough surface based on parabolic equation

Dong-Min Zhang(张东民), Cheng Liao(廖成), Liang Zhou(周亮), Xiao-Chuan Deng(邓小川), Ju Feng(冯菊)
Chin. Phys. B . 2018, 27(7): 074102. **doi:** 10.1088/1674-1056/27/7/074102

Influence of cutting off position of plasma filament formed by two-color femtosecond laser on terahertz generation

Zhan-Qiang Xue(薛占强), Li-Ping Shang(尚丽平), Hu Deng(邓琥), Qian-Cheng Zhang(张前成), Quan-Cheng Liu(刘泉澄), Wei-Wei Qu(屈薇薇), Zhan-Feng Li(李占锋), Shun-Li Wang(王顺利)
Chin. Phys. B . 2018, 27(5): 054101. **doi:** 10.1088/1674-1056/27/5/054101

Confinement of Bloch surface waves in a graphene-based one-dimensional photonic crystal and sensing applications

Xiu-Juan Zou(邹秀娟), Gai-Ge Zheng(郑改革), Yun-Yun Chen(陈云云)
Chin. Phys. B . 2018, 27(5): 054102. **doi:** 10.1088/1674-1056/27/5/054102

Design of scale model of plate-shaped absorber in a wide frequency range

Li-Ming Yuan(袁黎明), Yong-Gang Xu(许勇刚), Wei Gao(高伟), Fei Dai(戴飞), Qi-Lin Wu(吴琪琳)
Chin. Phys. B . 2018, 27(4): 044101. **doi:** 10.1088/1674-1056/27/4/044101

Ultra-thin single-layer transparent geometrical phase gradient metasurface and its application to high-gain circularly-polarized lens antenna

Tang-Jing Li(李唐景), Jian-Gang Liang(梁建刚), Hai-Peng Li(李海鹏), Ya-Qiao Liu(刘亚峤)
Chin. Phys. B . 2016, 25(9): 094101. **doi:** 10.1088/1674-1056/25/9/094101

Ultra-thin circularly polarized lens antenna based on single-layered transparent metasurface*

Kaiyue Liu(刘凯越), Guangming Wang(王光明)†, Tong Cai(蔡通)‡,
Wenlong Guo(郭文龙), Yaqiang Zhuang(庄亚强), and Gang Liu(刘刚)

Air Force Engineering University, Xi'an 710051, *China*

(Received 26 February 2018; revised manuscript received 16 April 2018; published online 25 July 2018)

Circularly polarized (CP) lens antenna has been applied to numerous wireless communication systems based on its unique advantages such as high antenna gain, low manufacturing cost, especially stable data transmission between the transmitter and the receiver. Unfortunately, current available CP lens antennas mostly suffer from high profile, low aperture efficiency as well as complex design. In this paper, we propose an ultra-thin CP lens antenna based on the designed single-layered Pancharatnam–Berry (PB) transparent metasurface with focusing property. The PB metasurface exhibits a high transmissivity, which ensures a high efficiency of the focusing property. Launched the metasurface with a CP patch antenna at its focal point, a low-profile lens antenna is simulated and measured. The experimental results show that our lens antenna exhibits a series of advantages including high radiation gain of 20.7 dB, aperture efficiency better than 41.3%, and also narrow half power beam width (HPBW) of 13°at about 14GHz. Our finding opens a door to realize ultra-thin transparent metasurface with other functionalities or at other working frequencies.

Keywords: lens antenna, ultra-thin, transparent Pancharatnam–Berry (PB) metasurface, single-layered

PACS: 41.20.Jb, 73.20.Mf **DOI:** 10.1088/1674-1056/27/8/084101

1. Introduction

Metamaterials[1–5] and their planar version, metasurfaces (MS), have provided strong capabilities to manipulate the wavefronts of electromagnetic (EM) waves through their desirable control on local phases. As a result, a lot of fascinating effects are investigated, such as anomalous refraction/reflection,[6–8] planar focusing lens,[9,10] photonic spin Hall effects,[11] propagation wave to surface wave[12,13] and many other related functional metadevices.[14,15] Very recently, Pancharatnam–Berry (PB) MS[6,16,17] have been proposed and studied to control circularly polarized (CP) waves in an effective way. Many multi-functional meta-devices have been designed by combining two sets of functional units, including bifunctional holograms[18] and multiplexing vortex beams.[19,20] However, the efficiencies of transmission-mode PB MS are typically very low because of the large specular modes. In practice, transmission geometry is more useful. Therefore, how to design a high-efficiency transmissive PB metasurface remains as a great challenge.

As one of the most important aspects, MS have been used to improve antenna performances. For example, primary antennas are engineered with a significant directivity enhancement by loading a multilayer focusing MS.[21–23] Four-beam antennas are also engineered by introducing phase-optimized MS.[24] However, the design of ultra-thin single-layered CP lens antenna has been reported rarely.

To solve these issues, in this paper, we propose a new strategy to improve the efficiency of transmissive PB MS by introducing anisotropic structures in a single-layered element. The simulated transmission amplitude reaches more than 0.9 for our designed element at its center frequency 14 GHz. To practically demonstrate the high efficiency of the proposed element, we design an ultra-thin transparent lens with a focal length of 40 mm. Excited by a well-optimized right hand circularly polarized (RHCP) patch antenna at the focal spot, a CP lens antenna is engineered and measured. Our study is useful to design other wave-manipulated meta-devices with high efficiencies.

2. Cell design

In order to provide a full control of the wave front, it is of great importance to obtain a complete phase variation in the whole range from 0 to 2π, while sustaining equal amplitude. Based on the PB theory,[6] we can manipulate the phase profile by rotating the structures while maintain a consistent amplitude information. An early theoretical study has claimed that working efficiency is bounded by 25% in transmissive ultra-thin MS.[25] Zhou[26] adopts an ABA transparent system to improve the efficiency and the experimental result is better than 90%. However, the structures are complex and suf-

*Project supported by the National Natural Science Foundation of China (Grant No. 61372034).
†Corresponding author. E-mail: wgming01@sina.com
‡Corresponding author. E-mail: caitong326@sina.cn
© 2018 Chinese Physical Society and IOP Publishing Ltd

fer from a multilayer system. Therefore, we propose a single-layered PB cell, which eliminates the drawbacks of multilayer.

As we know, a RHCP wave propagating along the +z direction and its transmitted waves can be described as follows:

$$\boldsymbol{E_i} = E_0(\hat{a}x - \mathrm{j}\hat{a}_y)\mathrm{e}^{-\mathrm{j}\boldsymbol{k}z}, \tag{1a}$$

$$\boldsymbol{E}_t^0 = E_0(\hat{a}xt_x\,\mathrm{e}^{\mathrm{j}\Phi_x} - \mathrm{j}\hat{a}yt_y\,\mathrm{e}^{\mathrm{j}\Phi_y})\mathrm{e}^{-\mathrm{j}\boldsymbol{k}z}, \tag{1b}$$

where $\boldsymbol{E}_i$ represents incident wave and $\boldsymbol{E}_t^0$ is the transmission wave with rotation angle of 0. E_0 is the amplitude of the transmitted wave. t_x (t_y) and Φ_x (Φ_y) stand for the transmissivity and the phase shift of x-(y-) polarized wave, respectively. k is the wave number. The transmitting matrix can be depicted as

$$T = \begin{pmatrix} t_x\,\mathrm{e}^{\mathrm{j}\Phi_x} & 0 \\ 0 & t_y\,\mathrm{e}^{\mathrm{j}\Phi_y} \end{pmatrix}. \tag{2}$$

Supposing $t_x = t_y = t$ and $\Phi_y = \Phi_x + \pi$, the transmission wave passing through the element rotated with angle of φ can be described as

$$\begin{aligned} \boldsymbol{E}_t^{\varphi} &= tE_0\big[\left(\cos\varphi\,\mathrm{e}^{\mathrm{j}\Phi_x} - \mathrm{j}\sin\varphi\,\mathrm{e}^{\mathrm{j}\Phi_x}\right)\hat{a}x \\ &\quad + \left(\sin\varphi\,\mathrm{e}^{\mathrm{j}\Phi_x} + \mathrm{j}\cos\varphi\,\mathrm{e}^{\mathrm{j}\Phi_x}\right)\hat{a}y\big]\,\mathrm{e}^{-\mathrm{j}\varphi}\mathrm{e}^{-\mathrm{j}\boldsymbol{k}z} \\ &= tE_0\,(\hat{a}x + \mathrm{j}\hat{a}_y)\,\mathrm{e}^{\mathrm{j}\Phi_x}\,\mathrm{e}^{-\mathrm{j}2\varphi}\mathrm{e}^{-\mathrm{j}\boldsymbol{k}z}. \end{aligned} \tag{3}$$

It can be seen that when the cell meets the demand of $t_x = t_y = t$ and $\Phi_y = \Phi_x + \pi$. The acquired phase discontinuity is twice that of the rotation angle of the element. The cells transmissive responses for x- and y-polarized waves should be

$$T = t\,\mathrm{e}^{\mathrm{j}\varphi_0}\begin{pmatrix} 1 & 0 \\ 0 & -1 \end{pmatrix}. \tag{4}$$

Thus, to realize a high efficiency, t should be as close as 1 and the phase difference between the x- and y-polarized components should be π. Therefore, the key step to realize a high efficiency is to find a proper element satisfying the mentioned principle.

Figure 1 shows the structure of the proposed element. The identical metal patterns with thickness of 0.036 mm are etched on top and bottom layers, and separated by an F4B dielectric substrate with thickness $h = 1.6$ mm, dielectric constant $\varepsilon_r = 2.65$, and loss tangent $\tan\delta = 0.001$. The detailed geometrical parameters of the element are listed as $p = 6.8$ mm, $l_1 = 2.2$ mm, $l_2 = 1.86$ mm, $l_3 = 0.7$ mm, $r_1 = 2.8$, $\alpha = 45°$. The anisotropic structures at x and y axes can be used to control the transmission phases along different polarizations, which can be used to achieve a π phase difference. The outer ring in our design is used to tune the transmission amplitude. As shown in Fig. 1(b), with periodic conditions set in x and y directions as well as open condition in z direction, x- and y-polarized waves are respectively applied to shine the metasurface (periodic of elements) along $-z$ direction in CST Microwave Studio.

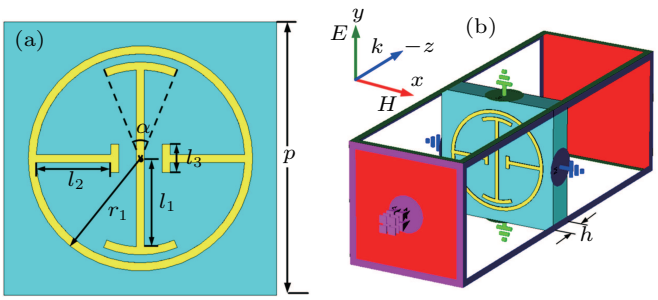


Fig. 1. (color online) Design and simulation of the element. (a) The structure of the element and (b) perspective view of the simulation setup.

To figure out the performance of the element, figures 2(a) and 2(b) accordingly plot the transmissivity and transmission phase for x- and y-polarized waves. Unanimously, the transmissivity under x- and y-polarizations reach more than 0.9 simultaneously, and the phase difference between Φ_x and Φ_y equals π approximately at 14 GHz, which exactly meet the requirements of high efficiency PB condition.

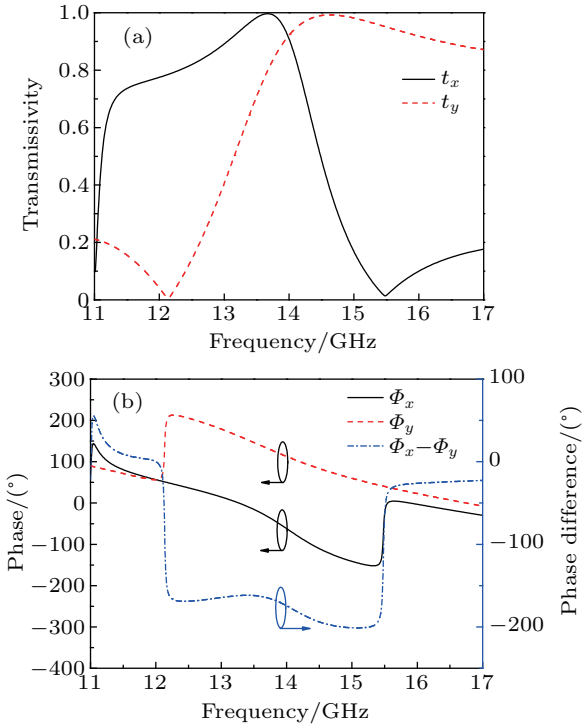


Fig. 2. (color online) The simulated (a) transmissivity and (b) phase shift of x-polarized and y-polarized plane waves.

Figure 3(a) shows the S parameters under RHCP wave illumination. We can see clearly that the element achieves a peak $|t_{\mathrm{LR}}|$ reaching 0.88 at 14 GHz and other modes ($|t_{\mathrm{RR}}|$, $|r_{\mathrm{LR}}|$, and $|r_{\mathrm{RR}}|$) are largely suppressed. Besides, as shown in Fig. 3(b), when rotated with different angles, the element exhibits phase shift satisfying $\Delta\Phi = 2\varphi$. Therefore, the proposed element is of highly transmitted efficiency and has the

capability of introducing abrupt phases with angular rotation to manipulate CP waves.

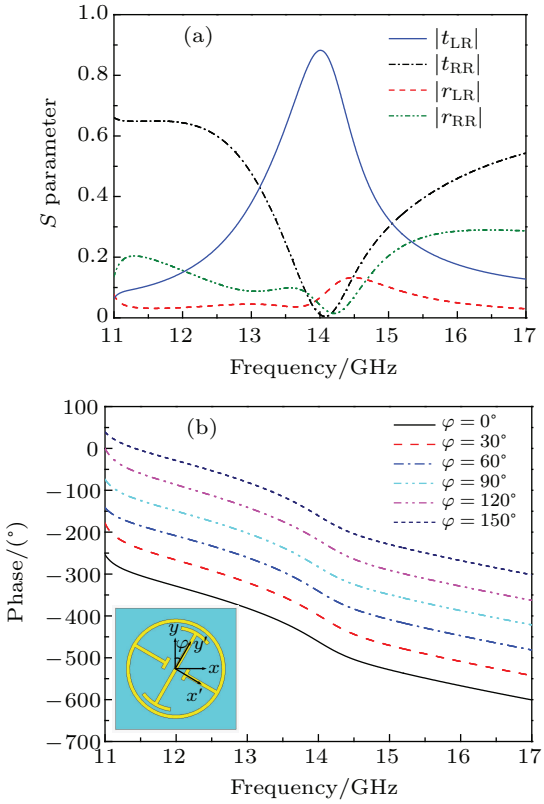


Fig. 3. (color online) (a) S parameters of the element under illumination of normally incident RCP wave. (b) phase shift of the element under different rotation angle.

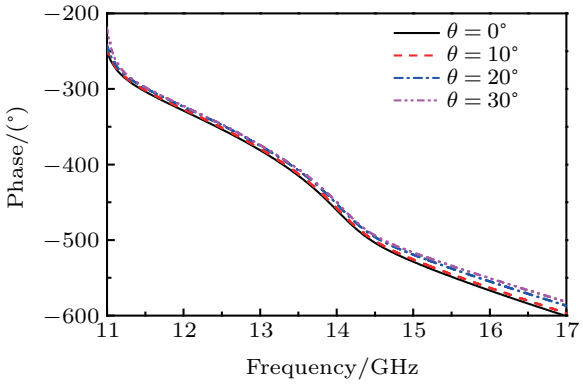


Fig. 4. (color online) phase shift under different incident angle θ.

To understand the transmission performance of the element under oblique incidence, figure 4 shows the transmission phase of the cross polarization component under different oblique incidence angles. The maximum phase discrepancy is about 10° at 14 GHz when the incident angle is 30°, which is acceptable and negligible in the following design.

3. Focusing MS design

With the well-optimized element in hand, we can design many functional meta-devices by manipulating the local phases of MS. Here, a focusing lens is designed for example. To achieve the goal of mentioned meta-lens, we require that the phase functions $\Phi(x,y)$ should satisfy the following parabolic distribution

$$\Phi(x,y) = \frac{2\pi}{\lambda}\left(\sqrt{x^2+y^2+F^2}-F\right)+\Phi_0. \tag{5}$$

Taking the element period into account, we can discretize the relative phase arrangement as

$$\Phi(m,n) = \frac{2\pi p}{\lambda}\left(\sqrt{m^2+n^2+(\frac{F}{p})^2}-\frac{F}{p}\right)+\Phi_0, \tag{6}$$

where p represents the element period and the parameters m and n are the number of elements along x and y directions, respectively. We set it as $F = 40$ mm for convenience. And $m = n = 15$ is chosen. Figure 5(a) shows the calculated phase distributions on the metasurface. Considering the relationship of compensated phases and rotation angles of elements, we design a meta-lens shown in Fig. 5(b), which occupies a size of 102 mm×102 mm. We characterize the property of the meta-lens by FDTD simulation. As depicted in Fig. 5(c), shining a RCP-polarized plane wave normally onto our metasurface at $f_0 = 14$ GHz with two measured lined set, we can obtain the E_x-field distributions at xoz and yoz planes with the results shown in Figs. 6(a) and (b). Obviously, good focusing effects are obtained at both planes, demonstrating the validity of our design. And the power flow distribution on xoz plane and xoy ($z = 40$ mm) planes as shown in Figs. 6(c) and (d) also prove the point.

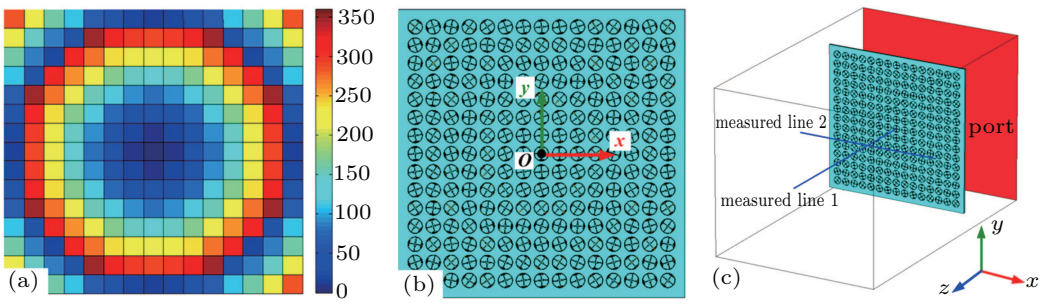


Fig. 5. (color online) Design of the transmissive MS. (a) Phase distribution, (b) top view of the MS, (c) simulation setup of the MS with e-field monitor and measured lines set to detect the focusing effect.

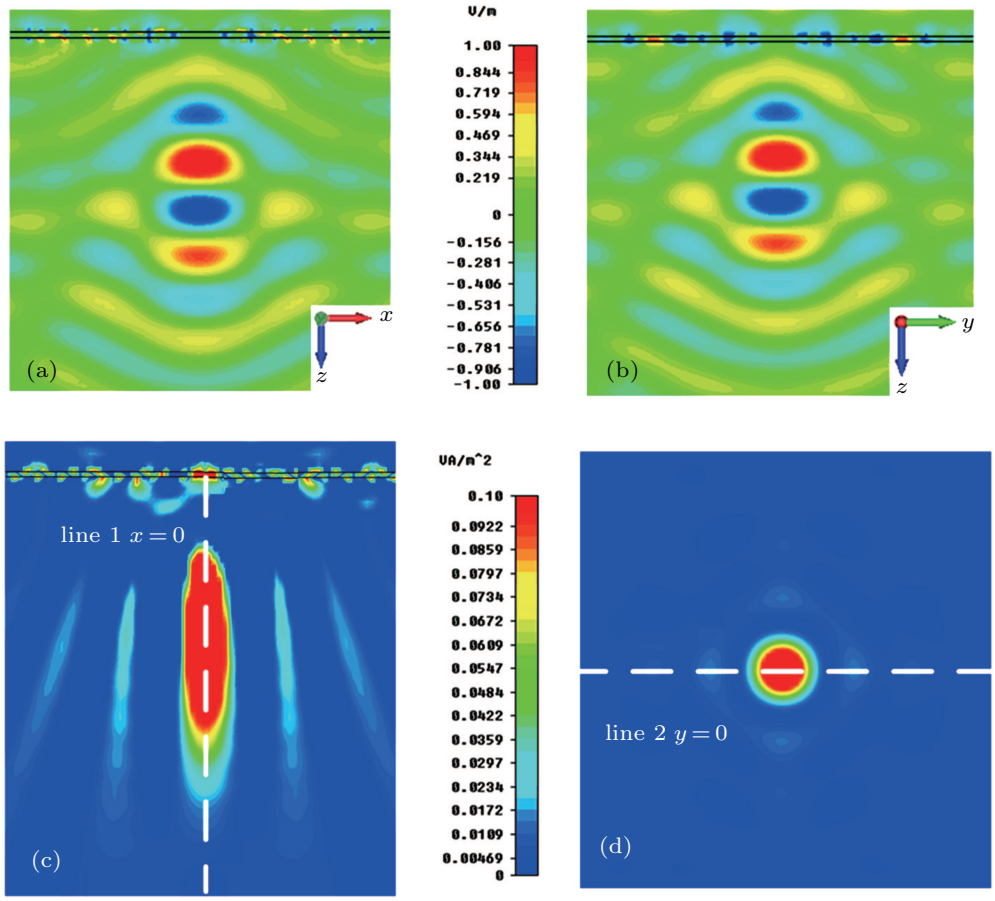


Fig. 6. (color online) Simulation results of the focusing MS under excitation of an RCP wave. Simulated Re(E_x) distributions on (a) *xoz* plane and (b) *yoz* plane. The power distributions at (c) *xoz* plane, and (d) *xoy* ($z = 40$ mm) plane.

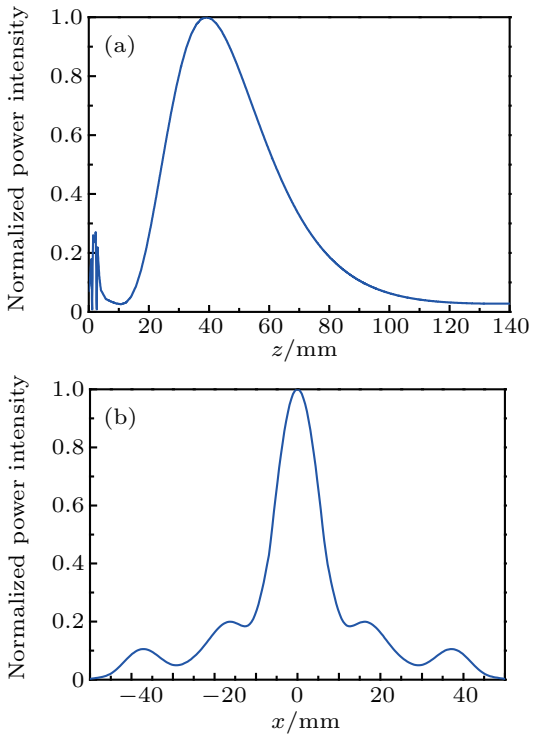


Fig. 7. (color online) Normalized power intensity distribution along (a) line 1 (b) line 2.

To give an insight into the focusing effect, we calculate and depict the power distributions along the measured line1 on *xoz* plane and measured line 2 on *xoy* plane shown in Fig. 7(a) and Fig. 7(b). The focal length is identified by the maximum value at z axis (shown in Fig. 7(a)) which is found as 40.94 mm. The simulated result coincides well with the design value. With the focal size defined as the half power width of the field intensity, we can find in Fig. 7(b) that the focal size of the MS is 12.59 mm (0.588λ) which is close to the theoretical limit 0.5λ.

4. Design of CP lens antenna

We can learn from the previous section that the designed meta-lens is capable of focusing a plane wave to a spot effectively. Based on the reciprocity of EM wave propagation, the meta-lens can also be employed to design CP antenna by converting the spherical wave emitted from the focal point into a plane wave. Thus, a CP patch antenna operating near 14 GHz is needed to act as the feed source. The CP patch antenna exhibits a 3-dB axial ratio (AR) bandwidth of 13.4 GHz–14.3 GHz, within which the antenna has a good impedance match property. By placing the patch antenna at the focal spot of the designed meta-lens, the CP lens antenna is designed with the structural configurations shown in Fig. 8(a). We simulated the 3D radiation pattern (Fig. 8(a)) at 14 GHz,

and the realized gain is about 20.9 dB. To prove the fact that our CP antenna can convert the quasi-spherical wave emitted by the source (see Fig. 8(b)) to plane wave. According to the E-field distribution of the lens antenna, flat wavefront at the transmission side of the meta-lens is observed clearly, which also explains the reason for the significantly increased radiation gain compared with the patch antenna. To further optimize the design of the lens antenna, the cases with different focal length to aperture diameter (F/D) are built and simulated. As shown in Figs. 8(d)–8(f), the simulated 3D far field radiation patterns are plotted for $F/D = 0.294$ ($F = 30$ mm), $F/D = 0.392$ ($F = 40$ mm), $F/D = 0.490$ ($F = 50$ mm). It is demonstrated that the lens antenna system obtains the highest gain when F/D is equals to 0.392 ($F = 40$ mm). Consequently, in the next study MS with focal length of 40 mm is selected as the research object.

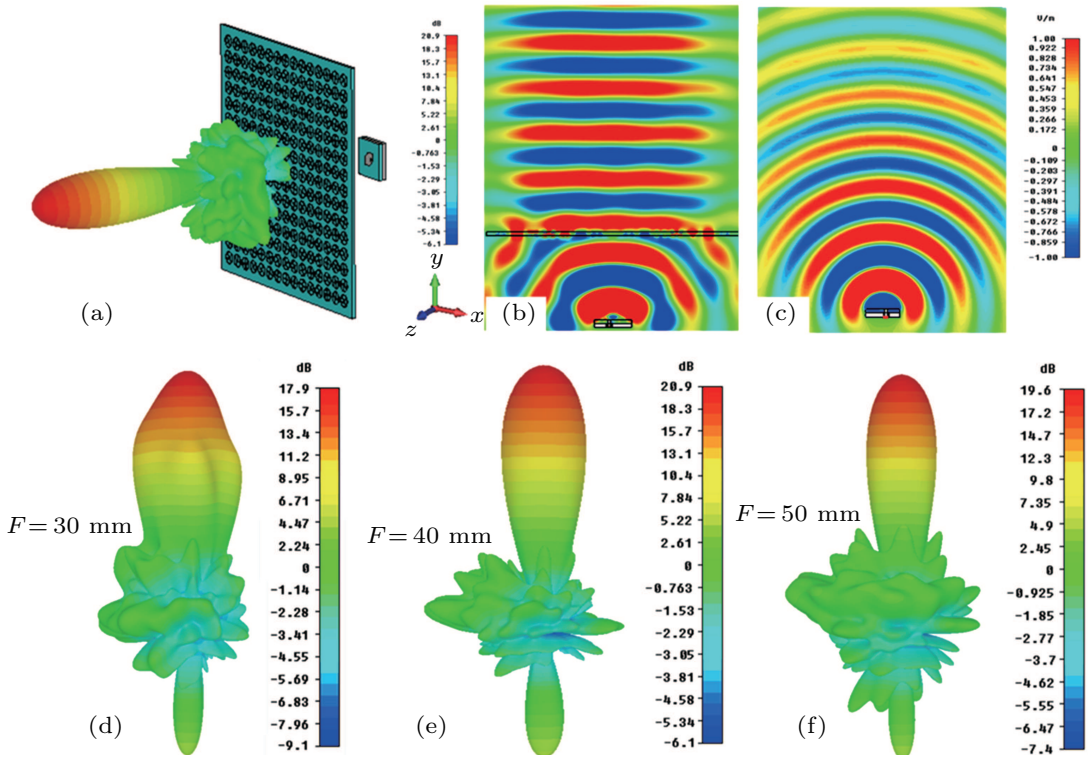


Fig. 8. (color online) Simulated results of the designed CP lens antenna. (a) 3D far-field radiation patterns. Re(E_x) distribution of lens antenna (b) with and (c) without MS. Radiation patterns for (d) $F = 30$ mm, (e) $F = 40$ mm, (f) $F = 50$ mm.

In order to verify the simulation, the MS and patch antenna are fabricated with their pictures shown in Fig. 9(a). The patch antenna and the MS are connected by four dielectric screws with length of 40 mm. The radiation patterns are measured in an anechoic chamber as depicted in Fig. 9(b).

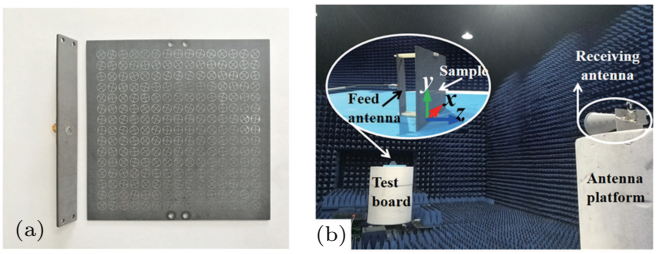


Fig. 9. (color online) Fabricated picture and measurement schematic of lens antenna. (a) Fabricated picture for MS and RCP antenna, (b) schematics of the far-field measurement.

Figures 10(a) and 10(b) plot the measured and simulated radiation patterns in *xoz*- and *yoz*-planes at 14 GHz for the patch antenna and lens antenna. It can be seen that a pencil beam is obtained for the lens antenna. Experimental results show that the measured gain is about 20.7 dB for the lens antenna, which is 12.8 dB higher than the patch antenna. Moreover, the half power beam width (HPBW) of is about 13° for our lens antenna. The aperture efficiency is one of the most important factors for the lens antenna, which is measured as 41.3% in our design, as shown in Fig. 10(d). Note that the obtained aperture efficiency is competitive than those of reported lens antennas.[27] Besides, to analyze the broadband characteristics of the lens antenna, the gain and AR performance in the frequency bandwidth of interest is also measured and then plotted in Fig. 10(c). It can be seen that at the center frequency the AR is 1.6 dB, and the 3-dB gain bandwidth is about 8.57% (13.4 GHz–14.6 GHz) while the measured 3-dB AR bandwidth is about 13.9% (13.3 GHz–15.3 GHz). To explain the properties of this work more clearly, a comparison table is given of recent lens antenna in Ref.[27] From Table 1, it is obvious that the aperture efficiency and AR of this paper at the center frequency have improved.

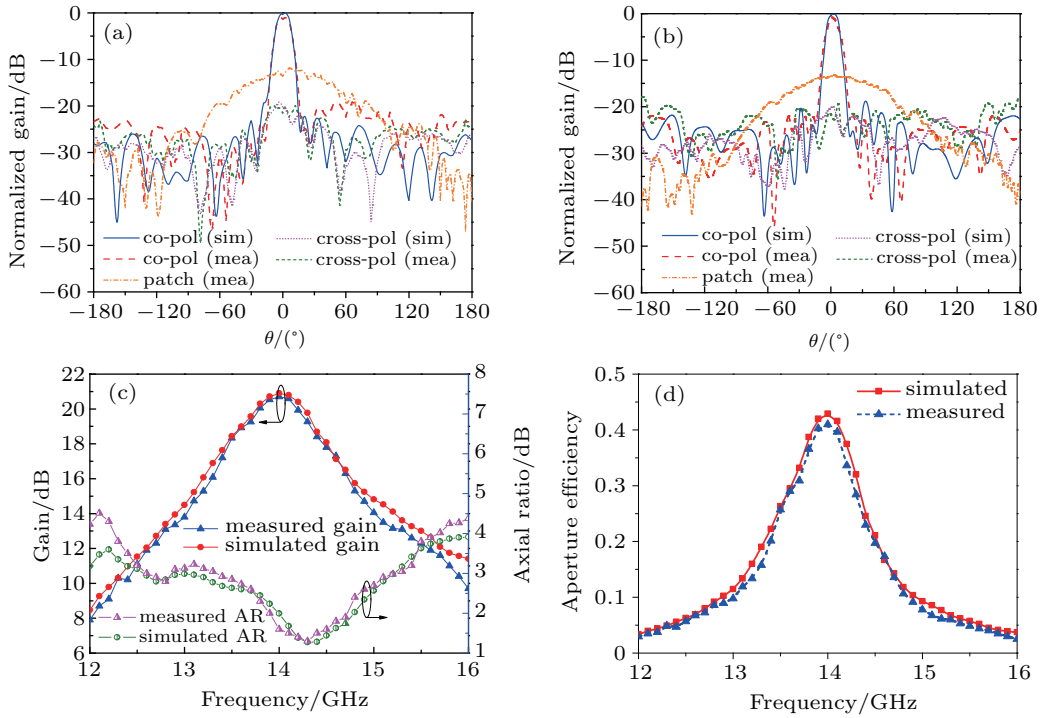


Fig. 10. (color online) Measured and simulated far-field radiation patterns in (a) *xoz*-plane (b) *yoz*-plane. Broadband performance of (c) gain and AR and (d) aperture efficiency.

Table 1. Comparison with previous work

	F/D	Frequency/GHz	Gain/dB	AR/dB	Aperture efficiency	3-dB AR bandwidth	3 dB-Gain bandwidth
This work	0.39	14	20.7	1.6	41.3%	8.57%	13.9%
Ref. [27]	0.32	13	17.6	2	41%	–	–

5. Conclusion and perspectives

In this paper, an ultra-thin CP lens antenna based on single-layered transparent metasurface is proposed, fabricated and measured. The MS consists of 15×15 cells with thickness of $0.07\lambda_0$ and takes up an area of 102 mm$\times$102 mm with $F/D = 0.39$. By placing an RCP radiating source at the focal point to launch the lens antenna, the quasi-spherical waves emitted from the patch antenna are efficiently transformed into plane waves, resulting in a high gain radiation in far field. The ultra-thin CP lens antenna achieves good radiation performances in terms of measured gain of 20.7 dB, aperture efficiency of 41.3%, HPBW of 13° at 14 GHz. Furthermore, the lens antenna effectively operates in the spectrum of 13.4 GHz–14.6 GHz. With improvements in efficiency, bandwidth, profile and layers reduction, our design may provide a promising approach to planar and integrate high gain CP antennas in wireless communication systems.

Acknowledgment

The authors would like to express their gratitude to anonymous reviewers for their helpful comments and China North Electronic Engineering Research Institute for the fabrication.

References

[1] Pendry J B, Holden A J, Robbins D J Z and Stewart W J 1998 *J. Phys.: Condens. Matter* **10** 4785
[2] Smith D R, Padilla J, Vier D C, Nemat-Nasser S C and Schultz S 2000 *Phys. Rev. Lett.* **84** 4184
[3] Xu H X, Wang G M, Qi M Q and Xu Z M 2012 *Appl. Phys. Lett.* **101** 173501
[4] Cai T, Wang G M and Liang J G 2017 *Appl. Phys. A* **123** 240
[5] Liu R P, Yang X M, Gollub J G, Mock J J, Cui T J and Smith D R 2009 *Appl. Phys. Lett.* **94** 073506
[6] Yu N F, Genevet P, Kats A, Aieta F, Tetienne J P, Capasso F and Gaburro Z 2011 *Science* **334** 333
[7] Sun S L, Yang K Y, Wang C M, Juan T K, Chen W T, Liao C Y, He Q, Xiao S Y, Kung W T, Guo G Y, Zhou L and Tsai D P 2012 *Nano Lett.* **12** 6223
[8] Zhang S, Park Y S, Li J, Lu X, Zhang W and Zhan X 2009 *Phys. Rev. Lett.* **102** 023901
[9] Zhang L, Gao S, Luo Q, Li W T, He Y J and Li Q X 2017 *IEEE Trans. Anten. Propag.* **65** 4529
[10] Zhang L, Wan X, Liu S, Yin J Y, Zhang Q, Wu H T and Cui T J 2017 *IEEE Trans. Anten. Propag.* **65** 3374
[11] Polina V K, Ginzburg P and Francisco J R F, *et al.* 2014 *Nat. Commun.* **5** 3226
[12] Sun S L, He Q, Xiao S Y, Xu Q, Li X and Zhou L 2012 *Nat. Mater.* **11** 426
[13] Wang J F, Qu S B, Ma H, Xu Z, Zhang A X, Zhou H, Chen H Y and Li Y F 2012 *Appl. Phys. Lett.* **101** 201104

[14] Liu R, Ji C, Mock J J, Chin J Y, Cui T J and Smith D R 2009 *Science* **323** 366
[15] Thakare Y B and Rajkumar 2010 *IET Microw. Anten. Propag.* **4** 175
[16] Cai T, Wang G M, Xu H X, Tang S W, Li H P, Liang J G and Zhuang Y Q 2017 *Ann. Phys.* 1700321
[17] Huang L, Chen X, Mühlenbernd H, Li G, Bai B, Tan Q, Jin G, Zentgraf T and Zhang S 2012 *Nano Lett.* **12** 5750
[18] Mueller J P, Rubin N A , Devlin R C , Groever B and Capasso F 2015 *Phys. Rev. Appl.* **118** 113901
[19] Liu Y C, Ke Y G, Zhou J X, Liu Y Y, Luo H L, Wen S C and Fan D Y 2017 *Sci. Rep.* **7** 40096
[20] Zhang K, Yuan Y Y, Zhang D W, Ding X M, Ratni B, Burokur S N, Lu M J, Tang K and Wu Q 2018 *Opt. Express* **26** 1351
[21] Cai T, Wang G M, Liang J G, Zhuang Y Q, Li T J 2017 *IEEE Trans. Anten. Propag.* **65** 3598
[22] Li H P, Wang G M, Xu H X, Cai T and Liang J G 2015 *IEEE Trans. Anten. Propag.* **63** 5144
[23] Guo W L, Wang G M, Li H P, Zhang K and Cai T 2016 *Chin. Phys. B* **25** 104101
[24] Payam N, Yang F and Elsherbeni Atef Z 2012 *IEEE Trans. Anten. Propag.* **60** 1166
[25] Ding X M, Monticone F, Zhang K, Zhang L, Gao D L, Burokur S N, Lustrac A D, Wu Q, Qiu C W and Alù A 2015 *Adv. Mater.* **27** 1195
[26] Luo W J, Sun S L, Xu H X, He Q, Zhou L 2017 *Phys. Rev. Appl.* **7** 044033
[27] Li T J, Liang J G, Li H P and Liu Y Q 2016 *Chin. Phys. B* **25** 094101